International Journal of Recent Development in Engineering and Technology
Website: www.ijrdet.com (ISSN 2347 - 6435 (Online)), Volume 2, Special Issue 3, February 2014)

International Conference on Trends in Mechanical, Aeronautical, Computer, Civil, Electrical and Electronics Engineering (ICMACE14)

A Novel Approach for Hyperspectral Image Mixed Noise Reduction Based on Improved K-SVD Algorithm

P. Thazneem Fazila[1], Dr. S. Kother Mohideen[2]

[1]*PG Student,* [2]*Assistant Professor, Computer Science and Engineering, National College of Engineering, Tirunelveli, Tamil Nadu, India*

***Abstract*—In this paper we deal with mixed noise reduction algorithm for Hyperspectral imagery (HSI). The hyperspectral data cube is considered as a three order tensor that is able to jointly treat both spatial and spectral modes. This entire denoising process is based on the K-SVD denoising algorithm. Our work involved in minimizing model to remove mixed noise such as Gaussian-Gaussian mixture, impulse noise and Gaussian-impulse noise from the HSI data. To solve the weighted rank-one approximation problem arisen from the proposed model, a new iterative scheme is given and the low rank approximation can be obtained by singular value decomposition(SVD) and we present a new weighting data fidelity function, which has the same minimize as the original likelihood functional but is much easier to optimize. The weighting function in the model can be determined by the algorithm itself, and it plays a role of noise detection in terms of the different estimated noise parameters.**

***Keyword* —Hyperspectral image, K-SVD algorithm, low rank approximation, Gaussian noise, Impulse noise, Mixed noise.**

I. INTRODUCTION

The 'Hyper' means 'over' and refers to a the large number of measured wavelength bands. HSI are spectrally over determined, which means it provides ample spectral information to identify and distinguish spectrally unique materials. The development of hyperspectral remote sensing technology makes it possible to provide large amount of spatial and spectral information for image analysis application such as classification, unmixing, subpixel mapping and target detection. However the acquired images are often distributed by radiometric noise such as sensor noise, photon noise calibration error, atmospheric scattering and absorption. The noise in these images can be categorized into two types: random noise and fixed–pattern noise. Fixed pattern noise is mostly due to calibration can be mitigated with suitable methods. In contrast, random noise cannot be removed entirely, due to its stochastic nature.

The random noise in HSI is the additive model, which is assumed to be white, Gaussian and independent-from-signal.

The traditional methods employ denoising algorithms such as singular value decomposition (SVD) and Wiener and wavelet filters, channel by channel. However these may lead to loss of the inter-dimensional information since they do not deal with the spatial and spectral information simultaneously .In recent years, some algorithm combine the spatial and spectral information for HSI noise reduction. A hybrid spatial spectral derivative domain wavelet shrinkage noise reduction (HSSNR) approach and spectral- spatial adaptive total variation model for hyperspectral image denoising was proposed.

In multilinear algebra, the HSI data cube can be considered as a three order tensor in which the spatial and spectral information are completely preserved. Examples of such approaches include multidimensional filtering based on tucker tensor decomposition. The multidimensional Wiener filtering (MWF) algorithm [13] is one of the Tucker based noise reduction which achieves simultaneous improvement in the image quality and classification accuracy. However this application may lead to information compression and loss of spatial details.

In the rank-1 tensor decomposition (R1TD) algorithm [24], the input data cube is considered as three order tensor. Subsequently, is used to extract the signal-dominant component from the observed HSI data cube by sorting the eigen values generated by tensor decomposition. The signal-dominant components are extracted from the observed data cube by sorting the weights of the rank-1tensor, and then they are reconstructed to produce the noise free image.

In this work, we propose a general framework to adaptively detect and remove noise of different type, including Gaussian noise, impulse noise and more importantly, their mixture in the HSI data. The HSI data is considered as a three order tensor which treats both spatial and spectral modes of the given image.

International Journal of Recent Development in Engineering and Technology
Website: www.ijrdet.com (ISSN 2347 - 6435 (Online)), Volume 2, Special Issue 3, February 2014)
International Conference on Trends in Mechanical, Aeronautical, Computer, Civil, Electrical and Electronics Engineering (ICMACE14)

The image undergoes tensor decomposition; later the modified K-SVD algorithm is applied to the tensors. We derive our model from the regularized maximum likelihood estimation (MLE) of the noise. Since the likelihood functional related to mixed noise is not easy to be optimized compared with the functional for a single Gaussian noise, a new functional with an additional variable is introduced. This new functional is easier to be optimized and has the same global minimizer (or maximizer) as the original likelihood functional. By minimizing the new functional, we obtain some weighted norms models, in which the weighting functions play the role of noise detectors. By integrating this with sparsity representation, our model can well restore images and textures corrupted by mixed noise. To solve the weighted rank-one approximation problem arisen from the proposed model, a new iterative scheme is given and the low rank approximation can be obtained by singular value decomposition (SVD). Our method integrates sparse coding-dictionary learning, image reconstruction, noise clustering (detection), and parameters estimation into a four step algorithm. Each step needs to solve a minimization problem. Then these optimized tensors are separated as noise free tensor and noisy tensor. The noise free tensors are then combined to reconstruct the noise free image. The reconstruction is same as reverse of the tensor decomposition.

The remainder of the study is organized as follows. Section2 deals with brief review about tensor and its operation. Section 3 proposed method and section 4 provides the experimental results. Finally, section 5 concludes this study.

II. Brief Review About HSI And Tensors

A. *Spectral image analysis*

To understand the advantages of hyperspectral imagery, it may help to first review some basic spectral remote sensing concepts. You may recall that each photon of light has a wavelength determined by its energy level. Light and other forms of electromagnetic radiation are commonly described in terms of their wavelengths. For example, visible light has wavelengths between 0.4 and 0.7 microns, while radio waves have wavelengths greater than about 30 cm (Fig. 1).Reflectance is the percentage of the light hitting a material that is then reflected by that material (as opposed to being absorbed or transmitted).

Some materials will reflect certain wavelengths of light, while other materials will absorb the same wavelengths. These patterns of reflectance and absorption across wavelengths can uniquely identify certain materials.

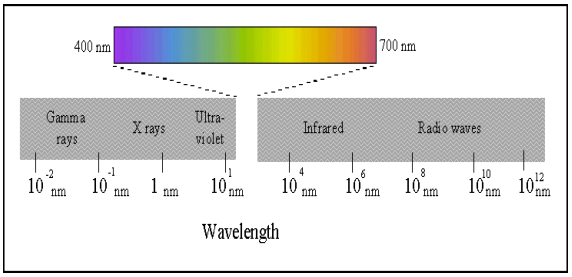

Fig 1 Electromagnetic Spectrum

B. *Imaging Techniques*

Depending on the number of spectral bands and wavelengths measured, an image is classified as a multispectral image when several wavelengths are measured and a hyperspectral image when a complete wavelength region, i.e., the whole spectrum, is measured for each spatial point. For example, a RGB image from a typical digital camera is a type of multispectral image that uses the light intensity at three specific wavelengths: red, green, and blue, to create an image in the visible region. The Fig 2 compares the optical information obtained by monochrome cameras, RGB cameras, and hyperspectral cameras.

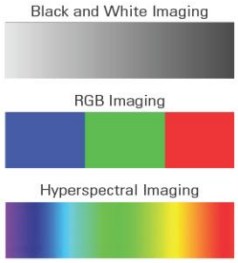

Fig 2 Differences in imaging

C. *Imaging spectrometer*

Hyperspectral images are produced by instruments called imaging spectrometers. The development of these complex sensors has involved the convergence of two related but distinct technologies: spectroscopy and the remote imaging of Earth and planetary surfaces.

International Journal of Recent Development in Engineering and Technology
Website: www.ijrdet.com (ISSN 2347 - 6435 (Online)), Volume 2, Special Issue 3, February 2014)
International Conference on Trends in Mechanical, Aeronautical, Computer, Civil, Electrical and Electronics Engineering (ICMACE14)

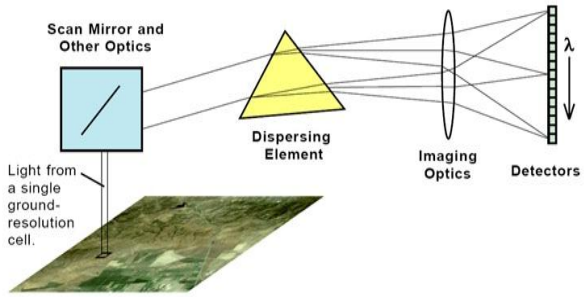

Fig 3 Imaging Spectrometer

Spectroscopy is the study of light that is emitted by or reflected from materials and its variation in energy with wavelength. As applied to the field of optical remote sensing, spectroscopy deals with the spectrum of sunlight that is diffusely reflected (scattered) by materials at the Earth's surface. Instruments called spectrometers (or spectroradiometers) are used to make ground-based or laboratory measurements of the light reflected from a test material. An optical dispersing element such as a grating or prism in the spectrometer splits this light into many narrow, adjacent wavelength bands and the energy in each band is measured by a separate detector. By using hundreds or even thousands of detectors, spectrometers can make spectral measurements of bands as narrow as 0.01 micrometers over a wide wavelength range, typically at least 0.4 to 2.4 micrometers (visible through middle infrared wavelength ranges).

Remote imagers are designed to focus and measure the light reflected from many adjacent areas on the Earth's surface. In many digital images, sequential measurements of small areas are made in a consistent geometric pattern as the sensor platform moves and subsequent processing is required to assemble them into an image.

D. Tensor

A tensor, represented as $A \in R^{L_1 \times L_2 \times \ldots\ldots \times L_N}$ is defined as a multidimensional array which is the higher-order equivalent of the vector (one-order tensor) and a matrix (two-order tensor). In this study, the HSI data cube is regarded as a three-order tensor $A \in R^{L_1 \times L_2 \times L_3}$ in which modes1 and 2 represent the spatial modes and mode 3 denotes the spectral mode. Taking each vector to be in different mode, we can visualize the outer product of three vectors as follows,

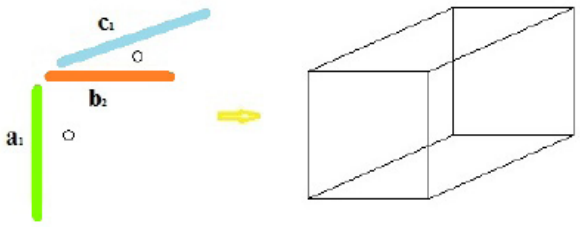

Fig 4 Tensor as the outer product of three vectors

International Journal of Recent Development in Engineering and Technology
Website: www.ijrdet.com (ISSN 2347 - 6435 (Online)), Volume 2, Special Issue 3, February 2014)
International Conference on Trends in Mechanical, Aeronautical, Computer, Civil, Electrical and Electronics Engineering (ICMACE14)

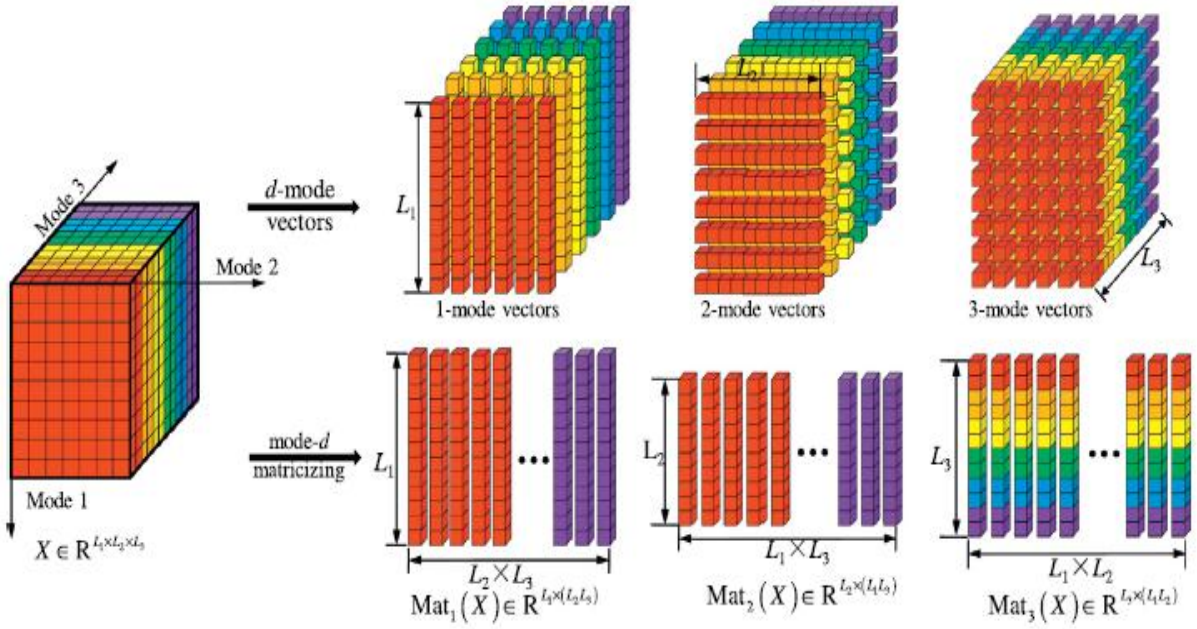

Fig 5 Illustration of tensor matricization of three modes

Mathematically, we can write the outer product of three vectors a; b; c as follows,

$$\begin{pmatrix} a_1 \\ a_2 \end{pmatrix} \circ \begin{pmatrix} b_1 \\ b_2 \end{pmatrix} \circ \begin{pmatrix} c_1 \\ c_2 \end{pmatrix} = \begin{matrix} a_1b_1c_2 & a_1b_2c_2 \\ a_2b_1c_2 & a_2b_2c_2 \end{matrix}$$
$$\begin{matrix} a_1b_1c_1 & a_1b_2c_1 \\ a_2b_1c_1 & a_2b_2c_1 \end{matrix}$$

We can see that the indexes of the entries in the resulting tensor.

Tensor matricization reorders the elements of an N-order tensor into a matrix from a given mode. The n-mode matricization of X belongs to $R^{L1 \times L2 \times \ldots \times LN}$ is matnX belongs to $R^{Li \times (L1L2 \ldots Ln-1\ Ln+1 \ldots LN)}$, which is the ensemble of vectors in the n-mode obtained by keeping index Li fixed and varying the other indices. A visual illustration of tensor matricization is shown in Fig 5.

III. METHODOLOGY

The given HSI is taken as input to the system. This HSI image is read and displayed. Then the HSI image processed in the R1TD algorithm to provide the Rank-1 Tensor profiles.

With these profiles, we perform the Alternative Least Square Algorithm to optimize the tensors. Then we sort the tensors of higher order and reconstruct the noise free image by combining signal dominant components.

A. HSI Image Reader

The Hyperspectral imaging (HSI) collects and process information from across the electromagnetic spectrum. Much as the human eye sees visible light in three bands (red, blue, green), spectral imaging divides the spectrum into many more bands. This technique of dividing images into bands can be extended before can be extended beyond the visibility. Hyperspectral sensors collect information as a set of 'images'. Each image represents a range of the electromagnetic spectrum and is also known as a spectral band. These 'images' are then combined and form a three dimensional hyperspectral data cube for processing and analysis. This module is designed to read and visualize the HSI images.

The HSI data is considered as multiple images combined as a cube. Thus we have view each image in a well furnished manner. Each image ahs slice of images of different colors.

International Journal of Recent Development in Engineering and Technology
Website: www.ijrdet.com (ISSN 2347 - 6435 (Online)), Volume 2, Special Issue 3, February 2014)
International Conference on Trends in Mechanical, Aeronautical, Computer, Civil, Electrical and Electronics Engineering (ICMACE14)

This slice of image is not taken as a single color image for the calculation instead it is taken as whole cube called tensors.

Here, we denote O as the observed HSI data cube consisting of the signal-dominant component S and the additive noise component N. By extending the classic two-dimensional additive noise model, the tensorial formulation is,

$$O=S+N \quad (1)$$

In this model, the noise is assumed to be white, Gaussian and independent from signal.

B. Tensor Decomposition

In this module, we develop a new tensor decomposition which jointly treats both the spatial and spectral modes. The R1TD algorithm is applied to the tensor data input which takes into account both the spatial and spectral information of the hyperspectral data cube. The tensor decomposition is of the form CANDECOMP/PARAFAC decomposition (Canonical decomposition and parallel factor decomposition).

The tensor decomposition was first attempted by Hitchcock in 1927 and Eckart and Young in 1936. However it was not fully introduced until 1970 with the work of Harshman about the PARAFAC decomposition of Carroll and Chang about CANDECOMP. Both paper appeared in Psychometrika and explained the same decomposition. The CANDECMOP/PARAFAC is based on the fact that tensors can be rewritten as the sum of the several other tensors. Since the outer product of the three vectors gives a tensor as a result. We shall denote this tensor to be of rank 1 and we will use the term "rank 1 tensor" to denote tensors that can be written as the outer product of the vector triple. The CANDECOMP/PARAFAC decomposition rewrites a given tensor as a sum of several rank 1 tensors. Following the argument above, we define a tensor to be rank 2 if it can be expressed as the sum of two rank 1 tensors. Similarly, we define a tensor to be of rank 3 if it can be expressed as the sum of three rank 1 tensors. Thus the definition of a rank of a tensor T is the minimal number of rank 1 tensors that yield T as a linear combination.

Based on the definitions of the rank 1 tensor and vector outer product, tensor $O \in R^{L_1 \times L_2 \times L_3}$ can be represented with the rank-1 tensor decomposition model:

$$O = \sum_{r=1}^{M} \lambda_r U_r \circ V_r \circ W_r \quad (2)$$

Where $U_r \in R^{L_1}, V_r \in R^{L_2}$ *and* $W_r \in R^{L_3}$ are vectors (rank-1 tensor in this model) on three modes, and M is the number of rank-1 tensors used to restore the whole tensor O. Considering λ_r as the weight value, the above implies that the HSI data is a linear combination of a sequence of rank-1 tensors. However, there is currently no straight forward solution to M or the so-called tensor rank. The rationale of this problem is explained as follows: The rank of a three order tensor is equivalent to the minimal number of triads necessary to describe the tensor.

C. Improved K-SVD algorithm

We, solve the following with four sub-minimization problem.

1) *Sparse Coding and Dictionary Learning:* The first minimization problem is

$$(\alpha^{\nu+1}, D^{\nu+1}) = \arg\min_{\alpha,D} \mathcal{J}(\alpha, D, f_\nu, u_\nu, \Theta_\nu) \quad (3)$$

Applying the alternating algorithm again to this subproblem, this problem can be split into two convex subproblems corresponding to the so-called sparse coding step and the dictionary learning step, respectively. Let $\nu 1$ be an inner iteration number, then $\alpha_{\nu+1,}$ and $D_{\nu+1}$ can be obtained by solving the following two minimization problems iteratively:

Sparse Coding (Conjugated OMP)

$$\alpha^{\nu_1+1} = \arg\min_{\alpha} \mathcal{J}(\alpha, D, f_\nu, u_\nu, \Theta_\nu)$$

$$= arg \min_{\alpha} \left\{ \frac{\lambda}{2} \sum_{i=1}^{N} \left\| W_i D^{\nu_1} \alpha_{.,i} - W_i R_i f^{\nu} \right\|_2^2 + \sum_{i=1}^{N} \mu_i \left\| \alpha_{.,i} \right\|_0 \right\} \quad (4)$$

In the above, W_i is a diagonal matrix whose diagonal elements are $R_{i\omega}$.

Dictionary Learning: (Modified K-SVD)

The linear structure of K-SVD is significantly changed by the non-uniform weights. We denote

$$W = (R_{1\omega} \dots R_{N\omega}), X = (R_1 f \dots R_N f) \quad (5)$$

Then

$$D^{\nu_1+1} = \arg\min_{D, \|d_k\|_2=1} \{ \|W \circ (D\alpha^{\nu_1+1} - X^{\nu})\|_F^2 \} \quad (6)$$

International Journal of Recent Development in Engineering and Technology
Website: www.ijrdet.com (ISSN 2347 - 6435 (Online)), Volume 2, Special Issue 3, February 2014)
International Conference on Trends in Mechanical, Aeronautical, Computer, Civil, Electrical and Electronics Engineering (ICMACE14)

Similar to the K-SVD learning algorithm of [13], a natural approach to minimize each atom d_k from following energy:

$$d_k^{\nu_1+1} = \arg\min_{\|d_k\|_2=1} \left\| W \circ (E^k - d_k \alpha_{k,\cdot}^{\nu_1+1}) \right\|_F^2 \quad (7)$$

In the above, $E^k \triangleq X^\nu - \sum_{l=1,l\neq k}^{K} d_l^{\nu_1} \alpha_{l,\cdot}^{\nu_1+1}$. This problem is known as weighted approximation. An iterative algorithm [22] to address this difficulty is as follows

$$d_k^{\nu_1+1} = \arg\min_{\|d_k\|_2=1} \left\| W \circ \left(E^k - d_k \alpha_{k,\cdot}^{\nu_1+1}\right) + d_k^{\nu_1} \alpha_{k,\cdot}^{\nu_1+1} - d_k \alpha_{k,\cdot} \right\|_F^2 \quad (8)$$

via SVD. This algorithm cannot be used for the unweighted case. Thus we solve the minimization problem was:

$$d_k^{\nu_1+1} = \arg\min_{\|d_k\|_2=1} \left\| W \circ \left(E^k - d_k \alpha_{k,\cdot}^{\nu_1+1}\right) + \tau_k d_k^{\nu_1} \alpha_{k,\cdot}^{\nu_1+1} - \tau_k d_k \alpha_{k,\cdot} \right\|_F^2 \quad (9)$$

To update the atoms, where $\tau_k = (d_k^{\nu_1})^T \left(\frac{\sum_{i=1}^N W_i}{N}\right) d_k^{\nu_1}$. Thus the modified scheme reduces the original K-SVD algorithm when all weights are the same.

Incorporating the sparse constraint, we get ourmodified K-SVD algorithm for weighted norm as follows:

1) Select the index set of patches S_kThat use atom d_k

$$S_k = \{i : \alpha_{k,i}^{\nu_1+1} \neq 0, i \leq i \leq N\}. \quad (10)$$

2) Let $\tau_k = (d_k^{\nu_1})^T \left(\frac{\sum_{i=1}^N W_i}{N}\right) d_k^{\nu_1}$, for each image patch with index i∈ S_k calculate the residual $e_i^{\sim k} = W_i \left(R_i f^\nu - D^{\nu_1} \alpha_{\cdot,i}^{\nu_1+1}\right) + \tau_k d_k^{\nu_1} \alpha_{k,i}^{\nu_1+1}$

(11)

3) Set $\tilde{E}^k \in \mathbb{R}^{n_1 n_2 \times |S_k|}$ with its columns being the $e_i^{\sim k}$ and update $d_k^{\nu_1+1}$ by minimizing

$$(d_k^{\nu_1+1}, \beta^* = arg \min_{\|d_k\|_2=1,\beta} \left\| \tilde{E}^k - \tau_k d_k \beta^T \right\|_F^2 \quad (12)$$

where $\beta \in \mathbb{R}^{|S_k|}$. This rank-one approximation can be solved using SVD decomposition of $\tilde{E}^k$

4) Replace $\alpha_{k,i}^{\nu_1+1}, i \in S_k$ by relevant elements of β^*.

In our experiment, we choose the inner iteration number $\nu_1 = 10$.

2) *Reconstruction:* The minimization problem we have to solve is as follows, since $\mathcal{J}$ is quadratic with respect to f, thus

$$f^{\nu+1} = \left(d(\omega \circ \omega) + \lambda \sum_{i=1}^{N} R_i^T d((R_i\omega) \circ (R_i\omega)) R_i \right)^{-1} \times \left(d(\omega \circ \omega) g + \lambda (\textstyle\sum_{i=1}^N R_i^T d((R_i\omega) \circ (R_i\omega)) R_i) \times D^{\nu+1} \alpha_{\cdot,i}^{\nu+1} \right) \quad (13)$$

Where $d(\omega \circ \omega)$ represents $diag(\omega \circ \omega)$ and R_i is a diagonal matrix. Thus the inverse matrix can be directly obtained.

3) *Noise Clustering* (Exception Step): The minimization problem we need to solve is $u^{\upsilon+1}$ and it can be computed by

$$u_{\cdot,l}^{\nu+1} = \frac{\frac{r_1^\nu}{\sigma_1^\nu} \exp(-T_l)}{\sum_{s=1}^{M} \frac{r_s^\nu}{\sigma_s^\nu} \exp(-T_s)} \quad (14)$$

4) Parameter Estimation: The minimization for this step is

$$\Theta^{\nu+1} = \arg\min_{\Theta, \sum r_l = 1} \mathcal{J}(\alpha^{\nu+1}, \mathbf{D}^{\nu+1}, f^{\nu+1}, \mathbf{u}^{\nu+1}, \Theta) = \arg\min_{\Theta, \sum r_l = 1} \left\{ \begin{array}{l} \frac{\lambda}{2} \sum_{i=1}^{N} ||\mathbf{R}_i w \circ (\mathbf{D}^{\nu+1} \alpha_{\cdot,i}^{\nu+1} - \mathbf{R}_i f^{\nu+1})||_2^2 \\ + < \mathbf{u}^{\nu+1} + \lambda \sum_{i=1}^{N} \mathbf{R}_i \mathbf{u}^{\nu+1}, \mathbf{1} > \ln \frac{\sigma_l}{r_l} \\ + \frac{1}{2} ||w \circ (g - f^{\nu+1})||_2^2 \end{array} \right\} \quad (15)$$

From equation $\frac{\partial \mathcal{J}}{\partial \Theta} = 0$, we get the closed-form solution of $\Theta^{\nu+1}$:

$$r_l^{\nu+1} = \frac{<u_{\cdot,l}^{\nu+1}, \mathbf{1}> + \lambda <\mathbf{M} u_{\cdot,l}^{\nu+1}, \mathbf{1}>}{<\mathbf{1}, \mathbf{1}> + \lambda <\mathbf{M}\mathbf{1}, \mathbf{1}>}$$

$$(\sigma_l^2)^{\nu+1} = \frac{<u_{\cdot,l}^{\nu+1}, (g - f^{\nu+1}) \circ (g - f^{\nu+1})>}{<u_{\cdot,l}^{\nu+1}, \mathbf{1}> + \lambda \sum_{i=1}^{N} <\mathbf{R}_i u_{\cdot,l}^{\nu+1}, \mathbf{R}_i \mathbf{1}>} + \frac{\lambda \sum_{i=1}^{N} <\mathbf{R}_i u_{\cdot,l}^{\nu+1}, (\mathbf{D}^{\nu+1} \alpha_{\cdot,i}^{\nu+1} - \mathbf{R}_i f^{\nu+1}) \circ (\mathbf{D}^{\nu+1} \alpha_{\cdot,i}^{\nu+1} - \mathbf{R}_i f^{\nu+1})>}{<u_{\cdot,l}^{\nu+1}, \mathbf{1}> + \lambda \sum_{i=1}^{N} <\mathbf{R}_i u_{\cdot,l}^{\nu+1}, \mathbf{R}_i \mathbf{1}>}. \quad (16)$$

International Journal of Recent Development in Engineering and Technology
Website: www.ijrdet.com (ISSN 2347 - 6435 (Online)), Volume 2, Special Issue 3, February 2014)

International Conference on Trends in Mechanical, Aeronautical, Computer, Civil, Electrical and Electronics Engineering (ICMACE14)

D. Denoising

The signal dominant components are combined leaving the noise tensors to the noise free image. After the noise components are removed, the signal-dominant components are obtained by reconstructing the remaining noise free tensor.

The tensors are reconstructed to form the noise free HSI data by the formula

$$\hat{S} = \sum_{r=1}^{k} \lambda_r U_r \circ V_r \circ W_r \quad (17)$$

The value of K is the number of signal dominant tensors.

IV. Experimental Results

The proposed algorithm is applied in 3 set of HSI data.

The HIS cannot be taken as an image itself. The values are to plotted as an image for our visualization. Thus a set of values of the received image is plotted as an image for our visualization. The values are plotted as an image for the original data and for the Denoised data. The original values are not plotted fully, only certain area shown for the visualization for a clear idea of the HSI image. The three images with their denoised output is shown in figure 6-8,

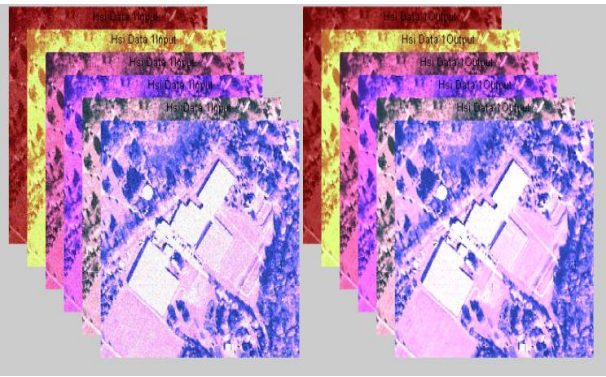

Fig 6 Data set 1 for HSI image visualization and the Denoised data set 1

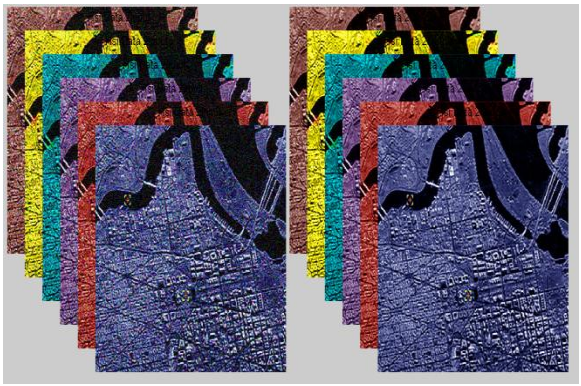

Fig 7 Data set 2 for HSI image visualization and the Denoised data set 2

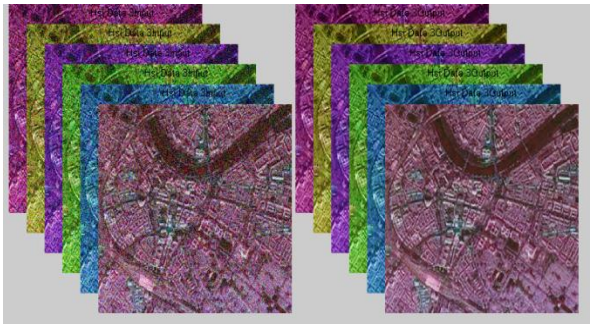

Fig 8 Data set 3 for HSI image visualization and the Denoised data set 3

To verify the effectiveness of the proposed algorithm, the proposed model is compared with several competitive methods: Spectral-Spatial Adaptive Total Variation (SSAHTV), Multidimensional Wiener Filtering (MWF) and Rank-1 Tensor Decomposition (R1TD). The algorithm SSAHTV [15] and MWF [13] may lead to loss of inter-dimensional information since the correlation between the spatial and spectral bands are not simultaneously considered. The application of a core tensor and n-mode tensor product may lead to information compression and loss of spatial details.

International Journal of Recent Development in Engineering and Technology
Website: www.ijrdet.com (ISSN 2347 - 6435 (Online)), Volume 2, Special Issue 3, February 2014)

International Conference on Trends in Mechanical, Aeronautical, Computer, Civil, Electrical and Electronics Engineering (ICMACE14)

The R1TD [24] provides clear view than that of the other two but it deals with only Additive white and Gaussian noise.

The proposed algorithm deals mixed noise like impulse, Gaussian-Gaussian, Gaussian-impulse. Also it provides a higher PSNR than that of the existing system.

The PSNR is an engineering term for ratio between the maximum possible power of a signal and the power of corrupting noise that affects the fidelity of its representation. Because many signals have a very wide dynamic range, PSNR is usually expressed in terms of logarithmic decibel scale.

The PSNR for the Existing System is compared with the proposed algorithm in the Table I. This comparison confirms that proposed method is has higher values than that of the existing systems. Also the existing system deals only with single noise whereas this deals with mixed noise.

TABLE I
PSNR COMPARISON FOR THE PROPOSED AND THE EXISTING SYSTEMS

PSNR Values				
Band No.	MWF	SSAHTV	R1TD	Improved K-SVD
1	24.48	28.40	30.39	36.51
2	24.66	26.44	30.43	34.42
3	25.48	28.43	30.43	31.75
4	24.31	28.21	30.20	33.58
5	24.73	29.02	29.99	34.36
6	23.73	27.56	29.52	31.14

The graph is plotted with the PSNR values provided in the table in figure 9.

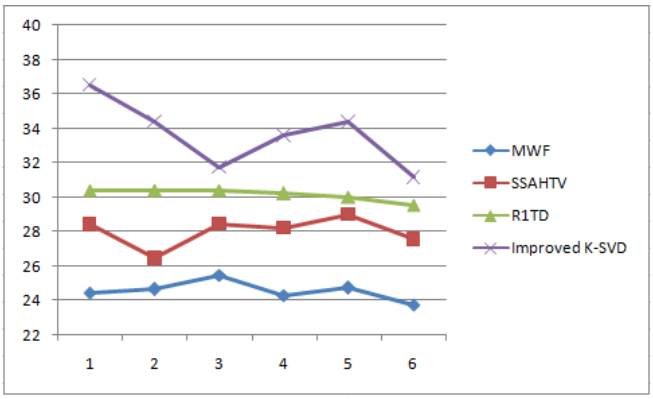

Fig 9 Graph providing the comparison of existing and the Proposed system.

V. CONCLUSION

We provide a general framework to remove mixed noise using the PDF. By combing the sparsity regularization and dictionary learning techniques, a novel and efficient model is designed to remove mixed noise such as Gaussian-Gaussian mixture, impulse noise and Gaussian plus impulse noise. Also it considers both spatial and spectral views of the hyperspectral image thus provide data quality in terms of both visual inspection and image quality.

REFERENCES

[1] Acito, N., Diani, M., Corsini, G., 2010. Hyperspectral signal subspace identification in the presence of rare signal components. IEEE Trans. Geosci. Remote Sens. 48 (4), 1940–1954.

[2] Acito, N., Diani, M., Corsini, G., 2011a. Signal-dependent noise modeling and model parameter estimation in hyperspectral images. IEEE Trans. Geosci. Remote Sens. 49 (8), 2957–2971.

[3] Acito, N., Diani, M., Corsini, G., 2011b. Subspace-based striping noise reduction in hyperspectral images. IEEE Trans. Geosci. Remote Sens. 49 (4), 1325–1342. Akaike, H., 1974.

[4] Ana Rovi., 2010. Analysis of 2× 2 × 2 Tensors. master's thesis

[5] M. Elad and M. Aharon, "Image denoising via learned dictionaries and sparse representation," in Proc. IEEE Comput. Vis. Pattern Recognit.,Jun. 2006, pp. 895–900.

[6] M. Elad and M. Aharon, "Image denoising via sparse and redundant representations over learned dictionaries," IEEE Trans. Image Process.,vol. 15, no. 12, pp. 3736–3745, Dec. 2006.

[7] M. Aharon, M. Elad, and A. Bruckstein, "The K-SVD: An algorithm for designing of overcomplete dictionaries for sparse representations,"IEEE Trans. Image Process., vol. 54, no. 11, pp. 4311–4322, Nov. 2006.

[8] J. Mairal, M. Elad, and G. Sapiro, "Sparse representation for color image restoration," IEEE Trans. Image Process., vol. 17, no. 1, pp. 53–69, Jan. 2008.

[9] Bourennane, S., Fossati, C., Cailly, A., 2011. Improvement of target-detection algorithms based on adaptive three-dimensional filtering. IEEE Trans. Geosci. Remote Sens. 49 (4), 1383–1395.

[10] Brett W. Bader and Tamara G. Kolda MATLAB Tensor Classes for Fast Algorithm Prototyping

[11] Bro, R., Kiers, H.A.L., 2003. A new efficient method for determining the number of components in PARAFAC models. J. Chemometr. 17 (5), 274–286Karami, A., Yazdi, M., Asli, A.Z., 2011. Noise reduction of hyperspectral images using kernel non-negative tucker decomposition. IEEE J. Sel. Top. Signal Process. 5 (3), 487–493.

[12] Landgrebe, D., 2002. Hyperspectral image data analysis. IEEE Signal Process. Mag. 19 (1), 17–28.

[13] Letexier, D., Bourennane, S., 2008. Noise removal from hyperspectral images by multidimensional filtering. IEEE Trans. Geosci. Remote Sens. 46 (7), 2061–2069.

[14] Othman, H., Qian, S.-E., 2006. Noise reduction of hyperspectral imagery using hybrid spatial–spectral derivative-domain wavelet shrinkage. IEEE Trans. Geosci. Remote Sens. 44 (2), 397–408.

[15] Yuan, Q., Zhang, L., Shen, H., 2012. Hyperspectral image denoising employing a spectral-spatial adaptive total variation model. IEEE Trans. Geosci. Remote Sens. 50 (10), 3660–3677.

[16] H. Wang and R. Haddad, "Adaptive median filters: New algorithms and results," IEEE Trans. Image Process., vol. 4, no. 4, pp. 499–502, Apr.1995.

[17] Y. Xiao, T. Zeng, J. Yu, and M. K. Ng, "Restoration of images corrupted by mixed Gaussian-impulse noise via l1-l0 minimization,"Pattern Recognit., vol. 44, no. 8, pp. 1708–1720, Aug. 2011.

[18] E. Lopez-Rubio, "Restoration of images corrupted by Gaussian

[19] and uniform impulsive noise," Pattern Recognit., vol. 43, no. 5,pp. 1835–1846, 2010.

[20] J. Liu, H. Huang, Z. Huan, and H. Zhang, "Adaptive variational method for restoring color images with high density impulse noise," Int. J.Comput. Vis., vol. 90, no. 2, pp. 131–149, 2010

[21] J. Bilmes. (1997). A Gentle Tutorial on the EM Algorithm and its Application to Parameter Estimation for Gaussian Mixture and Hidden Markov Models [Online]. Available: http://citeseerx.ist.psu.edu/viewdoc/summary?doi=10.1.1.28.613

[22] N. Srebro and T. Jaakkola, "Weighted low-rank approximations," in Proc. 20th Int. Conf. Mach. Learn., 2003, pp. 720–727.

[23] S. Ko and Y. Lee, "Center weighted median filters and their applications to image enhancement," IEEE Trans. Circuits Syst., vol. 38, no. 9, pp.984–993, Sep. 1991.

[24] Xian Guo a, Xin Huang a,⇑, Liangpei Zhang a, Lefei Zhang"Hyperspectral image noise reduction based on rank-1 tensor Decomposition", ISPRS Journal of Photogrammetry and Remote Sensing 83 (2013) 50–63